A Model of Cleavage Fracture along Metal/Ceramic Interfaces

D. M. LIPKIN*, G. E. BELTZ†, and D. R. CLARKE*
*Materials Department, †Department of Mechanical & Environmental Engineering, University of California, Santa Barbara, CA 93106

ABSTRACT

We propose a mechanism by which cleavage-type crack growth along a metal/ceramic interface could proceed concomitantly with significant plastic dissipation in the metal. The large strain gradients in the immediate vicinity of the crack tip are postulated to lead to extensive local hardening. A simple, continuum-based model is used to identify a characteristic length scale ahead of the crack tip, within which the material can not plastically deform subject to the crack-tip stress field. An analytical expression is derived for the crack-tip shielding afforded by the plastic zone. The coupling between the plastic dissipation and the ideal work of fracture is found to be synergistic, with slight variations in Griffith energy affecting order-of-magnitude changes in toughness. These results suggest a possible mechanism for a number of interfacial fracture phenomena observed in thick- and thin-film metal/ceramic systems, including segregation-induced interfacial embrittlement, the ductile-to-brittle transition, and stress corrosion cracking.

INTRODUCTION

A number of fracture processes exhibit superficial characteristics of cleavage fracture, while the corresponding fracture energy greatly exceeds the work of adhesion, implying extensive plastic dissipation. Early fracture models drew a sharp distinction between "brittle" and "ductile" fracture. Ideally brittle (or Griffith) fracture is identified with the energy to create fresh fracture surfaces [1], whereas fully plastic fracture is typically characterized by crack-tip blunting and hole growth [2,3]. Orowan's modification of the Griffith criterion to include the plastic work dissipated in the crack-tip process zone [4] was the first attempt to bridge the gap between ductile and brittle fracture models. However, Rice recognized that the plastic work dissipated during fracture has a strong functional dependence on the Griffith energy itself (the "valve" effect) [5]. The major subtlety of the valve effect is that the fracture events occur on vastly differing length scales: micron-scale plastic deformation at stresses near the yield strength and atomic-scale crack-tip decohesion at stresses approaching the cohesive strength of the solid.

Segregation-induced interfacial embrittlement in metal-ceramic couples [6-8] is a prime example of the strong role played by plastic dissipation in an otherwise cleavage-type fracture. Previous attempts at quantifying the valve effect, notably those by Thomson [9], Suo *et al.* [10] and Jokl *et al.* [11], have confirmed the inherently non-linear coupling between the crack-tip decohesion and the surrounding plastic deformation. However, these models fall short of a self-consistent description of the fracture process in terms of measurable material parameters. Recently, we presented an analysis for cleavage-type fracture in homogeneous materials [12], proposing a new methodology for describing the fracture process at all length scales. Presently, we extend this analysis to interfacial fracture in bimaterial systems. Employing concepts from strain-gradient plasticity and continuum asymptotic crack-tip field solutions, we obtain an inherent material length scale within which dislocation plasticity is inhibited. We ultimately arrive at the shielding ratio in terms of the interfacial work of adhesion, macroscopic toughness, yield strength, and work-hardening exponent.

THE MODEL

i. The Plastic Zone

Figure 1 illustrates the physical basis for the following discussion. A bimaterial couple containing a sharp interfacial crack is loaded in opening by remote tractions. For simplicity, we assume plane strain conditions. While the material in the lower half-plane is specified to be elastic, the upper half-plane is allowed to plastically deform and strain harden, such that a plastic zone develops about the crack tip. Following the small-strain limit of the generalized Ramberg-Osgood constitutive law:

Mat. Res. Soc. Symp. Proc. Vol. 436 © 1997 Materials Research Society

$$\bar{\sigma} = \sigma_o \left(\frac{E\bar{\varepsilon}_p}{\beta\sigma_o} \right)^n, \qquad (1)$$

where $\bar{\sigma}$ is the effective stress ($\bar{\sigma}^2 = 3/2\, s_{ij}s_{ij}$, where s_{ij} is the stress deviator), σ_o is the uniaxial yield stress, $\bar{\varepsilon}_p$ is the effective plastic strain ($\bar{\varepsilon}_p^2 = 2/3\, \varepsilon_{ij}\varepsilon_{ij}$), E is Young's modulus, n is the work-hardening exponent, and β is an empirical prefactor of order unity (β=3/7 in the original Ramberg-Osgood formulation [13]). The asymptotic stress field in the vicinity of the crack tip is taken from a modified HRR [14,15] solution presented by Wang [16], henceforth referred to as WHRR. To maintain continuity of tractions across the interface, Wang noted that the stresses over the entire region must have the same singularity. Taking the stress fields in both solids to be separable, the effective stress about the crack tip can therefore be expressed as:

$$\bar{\sigma} = \sigma_o \left(\frac{\xi}{\beta I_n} \frac{K_{I,\infty}^2}{r\sigma_o^2} \right)^{n/(1+n)} \tilde{\sigma}_e(\theta, n), \qquad (2)$$

where r is the distance ahead of the crack tip, $\xi = 1 - \nu^2$, ν is Poisson's ratio, and $K_{I,\infty}$ is the applied, or far-field, stress intensity factor that characterizes the elastic field well beyond the plastic zone. (We assume small-scale yielding, wherein the plastic zone remains small in relation to other length scales in the problem.) The factors $\tilde{\sigma}_e$ and I_n are weak functions of the work-hardening exponent, and are determined numerically in the WHRR formulation.† The requirement that the stress field be separable fixes the crack-tip mode mixity parameter, M_p, which is defined as $2/\pi \tan^{-1}(\tilde{\sigma}_{\theta\theta}(0)/\tilde{\sigma}_{r\theta}(0))$. The value of M_p is determined in the analysis. Figure 2 illustrates representative stress, strain, and displacement field solutions for n=0.3. Note that, aside from the discontinuity in the in-plane stresses across the interface, the fields in the elastic-plastic solid are quite similar to those of the homogeneous HRR solution [14].

ii. Crack-Tip Strain-Gradient Plasticity (HRR-type Field)

As for any asymptotic continuum formulation, the WHRR field does not extend to the very crack tip, being superseded by highly nonlinear behavior at the atomic length scale. As we have proposed in [12], however, the validity of conventionally accepted continuum asymptotic fields can break down at substantially larger-than-atomic length scales. The conjecture was based on recent work of Fleck *et al.* [17], who have shown that in the presence of large plastic strain gradients, conventional plasticity formulations must be severely modified at length scales far exceeding atomic dimensions (up to several microns). (More detailed discussion of the theoretical and experimental basis of strain-gradient plasticity is found in [17] and references therein.) On this basis, we have calculated an inherent distance within which the flow strength of the material exceeds the magnitude of the singular stress field of a crack. This parameter, which has hitherto been ill-defined in the application of strain-gradient plasticity theory to cracks, suggests a new approach for incorporating vastly different length scales into a unified fracture model.

Conventionally, the local flow strength of a plastically deforming material is related to the local dislocation density, ρ_T, through a modified Orowan-Taylor relation [18]:

$$\bar{\sigma}_{flow} = \alpha E b \sqrt{\rho_T}, \qquad (3)$$

where α is a constant prefactor of order unity and b is the Burgers vector. In conventional crystal hardening theory, all of the dislocations are "statistically stored," whether they existed prior to deformation or arose during deformation via various dislocation-generating sources. However, as argued by Ashby [19], an additional distribution of dislocations is "geometrically necessary" to maintain displacement compatibility in spatially gradient strain fields. The net dislocation density is therefore the sum of the statistically stored and geometrically necessary

† The fourth-order o.d.e. was solved on a Silicon Graphics workstation using a shooting method similar to that described in References 14 and 15.

densities ($\rho_T = \rho_G + \rho_S$). Where local strain gradients become large -- as occurs near crack tips -- the geometrically necessary dislocation density can far exceed the statistically stored contribution ($\rho_G >> \rho_S$), whereupon the flow strength in such regions can be approximated by substituting ρ_G into Eqn.3. For isotropic plasticity following J_2-deformation theory, the density of geometrically necessary dislocations is directly proportional to the effective curvature, χ_e:

$$\rho_G \approx \frac{\chi_e}{b}, \tag{4}$$

where $\chi_e = \sqrt{\frac{2}{3}\chi_{ni}^{pl}\chi_{ni}^{pl}}$ and the curvature tensor, χ^{pl}, is related to the plastic strain, ε^{pl}, through:§

$$\chi_{ni}^{pl} = e_{nkj}\,\varepsilon_{ij,k}^{pl}, \tag{5}$$

where e_{nkj} is the permutation tensor and $\varepsilon_{ij,k}^{pl} \equiv \partial\varepsilon_{ij}^{pl}/\partial x_k$.

The asymptotic strain field for a crack exhibiting a WHRR singularity is:

$$\varepsilon_{ij}^{pl} = \frac{\beta\sigma_o}{E}\left(\frac{\xi}{\beta I_n}\frac{K_{I,\infty}^2}{r\sigma_o^2}\right)^{1/(1+n)}\tilde{\varepsilon}_{ij}(\theta,n), \tag{6}$$

from which the effective curvature can be calculated [12]:

$$\chi_e = \sqrt{\tfrac{2}{3}}\frac{\beta\sigma_o}{E}\left(\frac{\xi}{\beta I_n}\frac{K_{I,\infty}^2}{r^{2+n}\sigma_o^2}\right)^{1/(1+n)}\tilde{\nabla}_e(\theta,n)\,, \tag{7}$$

where $\tilde{\nabla}_e^2 = \left(\frac{1}{1+n}\tilde{\varepsilon}_{r\theta} + \tilde{\varepsilon}_{rr,\theta}\right)^2 + \left(\frac{1}{1+n}\tilde{\varepsilon}_{\theta\theta} + \tilde{\varepsilon}_{r\theta,\theta}\right)^2$. (For clarity, the designation 'pl' has been omitted; henceforth, it is implicitly assumed that both the curvature tensor and strain components are associated with plastic deformation.) Combining Eqns.3, 4, and 7, we can identify the asymptotic strain-gradient-induced hardening distribution about the crack tip:

$$\bar{\sigma}_{flow} = \left(\tfrac{2}{3}\right)^{1/4}\alpha\sqrt{\beta\tilde{\nabla}_e\, b\sigma_o E}\left(\frac{\xi}{\beta I_n}\frac{K_{I,\infty}^2}{r^{2+n}\sigma_o^2}\right)^{1/2(1+n)}. \tag{8}$$

iii. The Core

From Eqn.8, we find that the rate of hardening due to geometrically necessary dislocations diverges as the crack tip is approached. For realistic values of the work-hardening exponent ($0<n<0.5$), the flow strength attains an approximately inverse-r singularity. Meanwhile, the WHRR asymptotic solution predicts that the stress field has *at most* an inverse-$\sqrt{r}$ singularity (LEFM), with no singularity whatsoever in the limit of perfect plasticity (Eqn.2). Thus, approaching the crack tip, the rate of increase of the flow strength exceeds the divergence of the stress field. *As a consequence, a point is reached at which material sufficiently close to the crack tip can no longer plastically deform under the prevailing crack-tip stress field.* The characteristic dimension thus defined is referred to as the crack-tip core.

In the absence of dislocation emission, the stress field inside the core retains an elastic singularity described by a crack-tip stress intensity factor, K_{tip}. (Note that the assumptions just made rely on the additional condition that the elastic core remains sufficiently larger than atomic dimensions for continuum elasticity theory to be valid.) The effective stress in the immediate vicinity of the crack tip can therefore be evaluated from linear-elastic fracture mechanics (LEFM):

§ Henceforth, Einstein summation convention over repeated indices is assumed.

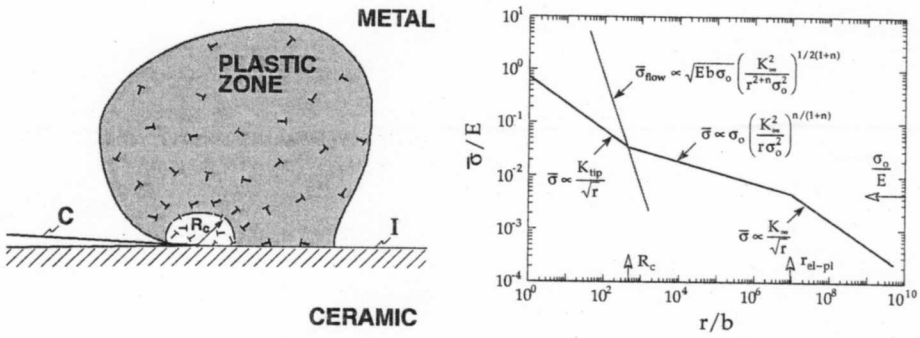

(a) (b)

Fig. 1 Illustration of the fracture model. (a) Plastic zone about a sharp interfacial crack (I=interface, C=crack). (b) Idealized stress distribution ahead of the crack tip. Approaching the crack tip, one moves from the far-field K-dominant region to the plastically deforming zone and finally to the core region. Stress continuity defines the location of the core boundary.

$$\bar{\sigma} = \lambda(\theta)\frac{K_{I,tip}}{\sqrt{r}}, \tag{9}$$

where the function λ conveys the angular dependence of the stress field ($4\pi\lambda^2 = [8\nu^2 - 8\nu + 5 - 3\cos(\theta)]\cos^2(\theta/2)$).

iv. Core Size and Shielding Ratio

It remains to establish the location of the boundary across which the scaling of the stress field switches from WHRR (Eqn.2) to LEFM (Eqn.9), and subsequently to evaluate the degree of crack-tip shielding afforded by the plastic zone.

At the point of incipient fracture, the crack-tip stress intensity must attain its critical value, K_c. Using the Irwin relation, we can restate the fracture criterion in terms of the critical energy release rate, $\mathcal{G}_c^{tip}$:

$$K_{I,tip} \rightarrow \sqrt{\tfrac{1}{\xi}\mathcal{G}_c^{tip}E}, \tag{10}$$

where $\mathcal{G}_c^{tip}$ is the Griffith toughness. The value of $\mathcal{G}_c^{tip}$ is simply the work of adhesion, W_{ad}, of the solid-solid interface -- a material parameter that can be calculated from atomistic models or estimated using various experimental techniques.

As seen from Fig.1b, the location of the interface corresponds to the crossover point at which the flow strength (Eqn.8) exceeds the stress attainable in a WHRR crack-tip field. (This empirical construction does not in itself guarantee compatibility, but has been used in limited circumstances to provide boundary conditions at elastic-plastic interfaces.) At distances closer to the crack tip than the core length, the stress is insufficient to induce plastic flow and the stress field is described by Eqn.9. Equations 2, 8 and 9 represent a system of three equations in three unknowns. Enforcing continuity of effective stress across the core boundary, $r = R_c$, along a fixed direction (say $\theta = 0$), we find that:

$$\frac{R_c}{b} = \left(\frac{g_n}{\tilde{\sigma}_e^2}\frac{E}{\sigma_o}\right)\left(\frac{\lambda^2}{g_n\xi}\frac{W_{ad}}{b\sigma_o}\right)^{1-2n} \tag{11}$$

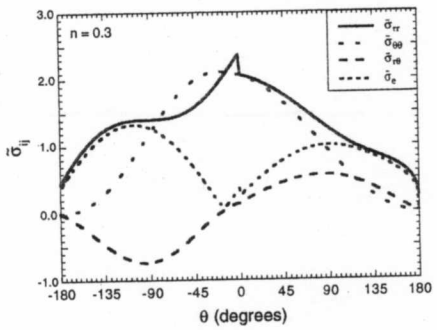

(a)

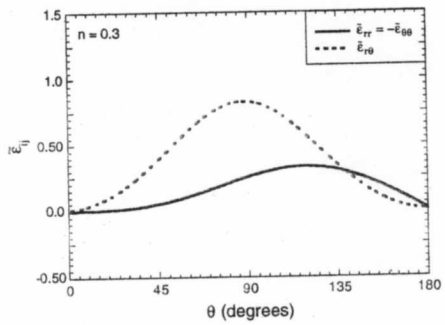

(b)

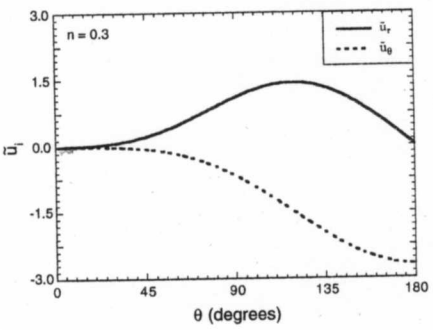

(c)

Fig. 2 The θ-variation of (a) stresses, (b) strains, and (c) displacements at the tip of a mode-I interfacial crack for n=0.3.

Table I. Selected values of plane strain WHRR parameters for $\theta = 0$.

n	M_p	$\tilde{\sigma}_e$	I_n	$\tilde{V}_e$
0.1	0.92	0.63	2.76	0.055
0.2	0.94	0.40	2.80	0.074
0.3	0.96	0.25	2.92	0.095
0.4	0.97	0.17	3.06	0.136
0.5	0.98	0.10	3.22	0.174

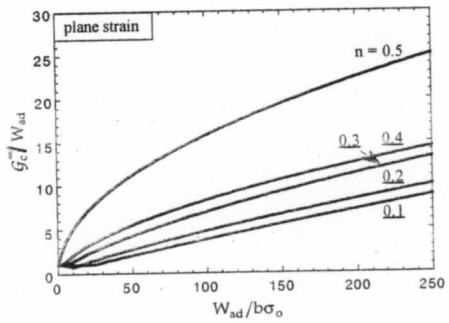

(a)

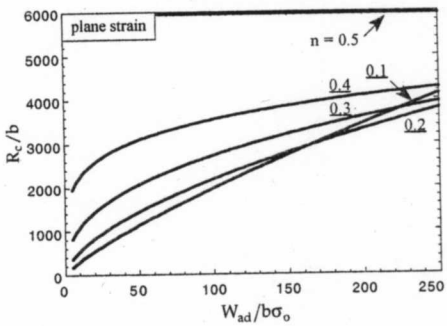

(b)

Fig. 3 Variation of (a) shielding ratio and (b) core size with the work of adhesion for a range of work-hardening exponents. α=1, β=3/7, ν=1/3, and E/σ_o=1000.

and

$$\frac{\mathcal{G}_c^{\infty}}{W_{ad}} = \left(\frac{\beta I_n}{\tilde{\sigma}_e^2}\frac{\lambda^2}{\xi}\right)\left(\frac{\lambda^2}{g_n\xi}\frac{W_{ad}}{b\sigma_o}\right)^{1-n}, \tag{12}$$

where $\mathcal{G}_c^{\infty}/W_{ad}$ defines the crack-tip shielding ratio and $g_n \equiv \sqrt{\frac{2}{3}}\alpha^2\beta\tilde{\nabla}_e$.

DISCUSSION

Using appropriate values for the proportionality constants in Eqns.11 and 12 (Table I), the core size and shielding ratio are plotted in Figs.3a and b, respectively, for a range of work-hardening exponents. The core size is generally much larger than the Burgers vector, suggesting that the use of continuum approximations of the prevailing fields is reasonable. The mode mixity parameter is nearly unity over the entire range of exponents considered, such that the loading is well approximated as mode I. The positive slopes of the shielding ratio curves in Fig.3a indicate that the strain-gradient model does predict a synergistic coupling between the macroscopic toughness (attributed to plastic deformation) and the inherent material toughness (represented by the ideal cleavage energy, W_{ad}). Such behavior is in qualitative agreement with observations of segregation-induced embrittlement [6-7], whence a slight reduction in the work of adhesion leads to a dramatic decrease in the macroscopic toughness. The magnitude of the shielding ratios appears to be approximately half of the respective values for the homogeneous fracture model [12]. This implies that, within the framework of the present model, the primary influence of the interface is to reduce the total volume of the plastic zone. The dimensionless material parameter, $W_{ad}/b\sigma_o$, can be utilized as a performance index for classifying the propensity for interfacial debonding in metal/ceramic systems.

REFERENCES

1. A.A.Griffith, *Phil.Trans.Roy.Soc.Lond. A* **221**, 163 (1920).
2. G.Hahn, M.Kanninen, and A.Rosenfeld, *Ann.Rev.Mater.Sci.* **2**, 381 (1970)
3. R.M.McMeeking, *J.Mech.Phys.Solids* **25**, 357 (1977).
4. E.Orowan, *Trans.Inst.Engrs.Shipbuilders Scot.* **89**, 165 (1945).
5. J.R.Rice, in *Proceedings of the 1st International Conference on Fracture*, (ed. by T.Yokobori, T.Kawasaki, and J.L.Swedlow), p.309. Sendai, Japan (1966).
6. D.Korn, G.Elssner, H.F.Fischmeister, and M.Rühle, *Acta metall.mater.* **40**, s355 (1992).
7. D.M.Lipkin, D.R.Clarke, and A.G.Evans, "Effects of Interfacial Segregation on Fracture in the Gold/Sapphire System," work in progress (1996).
8. J.R.Rice, Z.Suo, and J.-S.Wang, in *Metal-Ceramic Interfaces*, (ed. by M.Ruhle, A.G.Evans, M.F.Ashby, and J.P.Hirth), p.269. Pergamon Press, NY (1990).
9. R.Thomson, *J.Mater.Sci.* **13**, 128 (1978).
10. Z.Suo, C.F.Shih, and A.G.Varias, *Acta metall.mater.* **41**, 1551 (1993).
11. M.L.Jokl, V.Vitek, and C.J.McMahon Jr., *Acta metall.mater.* **28**, 1479 (1980).
12. D.M.Lipkin, D.R.Clarke, and G.E.Beltz, *Acta mater.*, in press (1996).
13. W.Ramberg and W.R.Osgood, NACA TN 902 (1943).
14. J.W.Hutchinson, *J.Mech.Phys.Solids* **16**, 13 & 337 (1968).
15. J.R.Rice and G.F.Rosengren, *J.Mech.Phys.Solids* **16**, 1 (1968).
16. T.C.Wang, *Engineering Fracture Mechanics* **37**[3], 527 (1990).
17. N.A.Fleck *et al.*, *Acta metall.mater.* **42**, 475 (1994).
18. M. Döner, H. Chang, H. Conrad, *JMPS* **22**, 555 (1974)
19. M.F.Ashby *et al.*, *Phil.Mag.* **21**, 413 (1970).